
Volume 1 | Number 1 | Jan 2013 | Pages 1–100
NJC
New Journal of Chemistry
www.rsc.org/njc
A journal for new directions in chemistry
ROYAL SOCIETY OF CHEMISTRY
cnrs

In situ spectroscopic study on decomposition of $MgSiO_3$ during alkali fusion process using sodium hydroxide

Min XU[1], *Zirui WANG*[1], *Qian XU*[1], *Qiushi SONG*[1], *Jinglin YOU*[2], *Yuchun ZHAI*[1]
[1]*School of Materials Science and Metallurgy, Northeastern University, Shenyang, 110004, PR China*
[2]*School of Material Science and Engineering, Shanghai University, Shanghai 200072, China,*

Abstract: The mechanism of decomposition of magnesium inosilicate ($MgSiO_3$) during the alkali fusion process using NaOH was investigated by Raman spectroscopy in situ and X-ray diffraction analyses. The results show that the tetrahedral silica chains within $MgSiO_3$ are gradually disrupted, and nesosilicate with the isolated SiO_4 tetrahedra becomes reorganized at the beginning of the alkali fusion process. In the decomposition of $MgSiO_3$, the two intermediates are Mg_2SiO_4 and Na_2MgSiO_4, while the final products are $Mg(OH)_2$ and Na_2SiO_4. It can be concluded that this decomposition did not initiate from the cation exchange reaction in the process.

Key words: Raman spectroscopy, alkali fusion, $MgSiO_3$, reaction pathway, reaction intermediate

1. Introduction

Garnierite (Ni, Mg)SiO_3 . nH_2O is an important constituent in nickel laterite deposits for bearing significant amounts of nickel. In general, silicate rich garnierite ores are amenable to pyrometallurgical processes to produce carbon ferro-nickel alloys, while nickel bound within genthite, clay and saprolite ores is processed by hydrometallurgical routes, such as atmospheric acid-leaching and high pressure acid-leaching methods. In recent years, owing to the lack of high grade nickel sources[1-5] several investigations have focused on the utilization of nickel silicate, primarily serpentine, although this contains less than 2wt% nickel. However, owing to the higher chemical and thermal stability of the silicate compared with the other nickel-bearing ores, more aggressive reaction conditions are required for the decomposition of garnierite. This in turn leads to a potentially higher energy consumption and a negative environmental impact. There have been some reports on the joint process of alkali-roasting activation and acid-leaching for extraction of the valuable components from silicate-bearing laterites in the environmentally sound manners [6-8]. The alkali-fusion process is an important operation, during which the strong bonds between the metal and silica components within the compound can be disrupted, then the metal atoms are released from the SiO_4 tetrahedral network. Therefore, it can lead to a high yield of nickel from the activated clinker by the subsequent acid-leaching process under moderate conditions.However, there are currently few reports on the mechanism of alkali activation for the silicate in detail, especially for the pathway of the reactions, although the starting materials and final products are usually known for the related chemical reactions. It is often difficult, if not impossible, to gather materials which represent reaction intermediates.

The Raman scattering measurement can be used as a fast, non-destructive and reliable method of the characterization of materials, and Raman spectroscopy has been applied extensively to monitor the chemical reactions. Investigation into changes in Raman mode frequencies with the elevated temperatures or pressures can provide the information on the

---

Corresponding author: E-mail: qianxu201@mail.neu.edu.cn , Tel.: +86-20-83684943. Fax: +86-24-83687731

chemical bonding characters and the crystal structures in the reaction mixture [9-12]. In this study, Raman spectra obtained in situ during the alkali fusion process were used to identify the presence of the intermediates of the reactions, and reveal the reaction pathway to the alkali fusion. Here, we used the synthetic magnesium metasilicate ($MgSiO_3$) instead of the natural garnierite, and examined binding changes and transient phase transformations occurring in the alkali-fusion by Raman spectroscopy in situ and X-ray diffraction analyses. Normally, within garnierite, magnesium metasilicate is the major composition, in which minor nickel substitutes magnesium. Their solid solutions of general formula $(Mg_{1-x}Ni_x)SiO_3$ are isomorphous. The mechanism of $(Mg,Ni)SiO_3$ decomposition during the alkali fusion process could analogically obtained form that of $MgSiO_3$. The typical Raman spectra with distinct sharp peaks of the colorless $MgSiO_3$ can be collected easily, which is another important reason why $MgSiO_3$ served as the subject of investigation in this study instead of the natural dark green garnierite. The darkly colored samples have traditionally been difficult to investigate using Raman spectroscopy because of their absorption of the excitation laser beam, causing thermal emission. This thermal emission appears as a broad band which is the featureless background superimposed over the range of the Raman spectrum, and precludes the observation of any typical vibration information.

2. Experimental methods

$MgSiO_3$ was prepared by the chemical precipitation method from analytical grade $MgCl_2$ and Na_2SiO_3 in the aqueous solution. The deposit was dried at 100 ℃, and then roasted at 1200 ℃ for 4 hours. Mg_2SiO_4 was synthesized by the solid reaction of $MgSiO_3$ prepared in this study and analytical grade MgO at 1200 ℃. The prepared $MgSiO_3$ and Mg_2SiO_4 were confirmed by X-ray diffraction examination. The alkali fusion process of $MgSiO_3$ with the various NaOH/ $MgSiO_3$ molar ratios was investigated in the homemade micro-furnace under different operating conditions by Raman spectroscopy in situ. Raman spectra were collected on the Raman spectrometer (Jobin Y'von LABRAM HR800). The pulsed exciting light (355 nm) from a Q-switch pulsed THG-Nd:YAG laster was focused by an Olympus BH-2 microscope, and the Raman scattering light from the reactants was collected by a confocal-len system. The spectral resolution was better than 2 cm^{-1} and the spatial resolution about 1μm. The Raman spectrometer was equipped with the intensive charge-coupled device (ICCD) to investigate the alkali fusion process. The cooled clinker of products of the alkali fusion process was washed by undistilled water at room temperature for several times. The undissolved residue was centrifugally separated from the solution and dried at room temperature, then roasted at 600 ℃ for the subsequent XRD analysis. Phase analyses of all the samples were carried out with a D/Max-2500PC X-ray diffractometer with Cu-Ka radiation.

3. Results and discussion

Fig. 1 shows the typical XRD patterns of the prepared $MgSiO_3$, and protoenstatite which is one of the three basic polymorphs [13] of $MgSiO_3$, and stable above ~1023 ℃. The result indicates the prepared $MgSiO_3$ is predominantly composed of protoenstatite since the $MgSiO_3$ deposit was roasted at 1200 ℃ in this study. The Raman spectra of the prepared $MgSiO_3$ at varied temperatures are shown in Fig.2. Raman spectra of the prepared $MgSiO_3$ are very much alike one another during the temperature changes from 20 to 600 ℃ other than the minor downward shift in all the frequency bands. In general, the inosilicates are characterized by (1) the Si-O-Si bending vibrations between 400 and 750 cm^{-1}, (2) the Si-O stretching vibrations between 800 and 1100 cm^{-1} (Q^n); and (3) metal-O bending vibrations below

600 cm^{-1}[14,15].

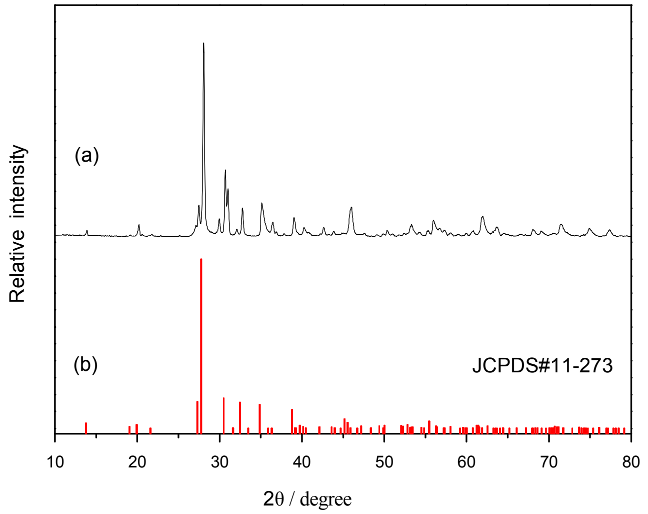

Fig.1 (a) XRD pattern of prepared $MgSiO_3$ and (b) standard XRD pattern of protoenstatite (JCPDS No.11-273)

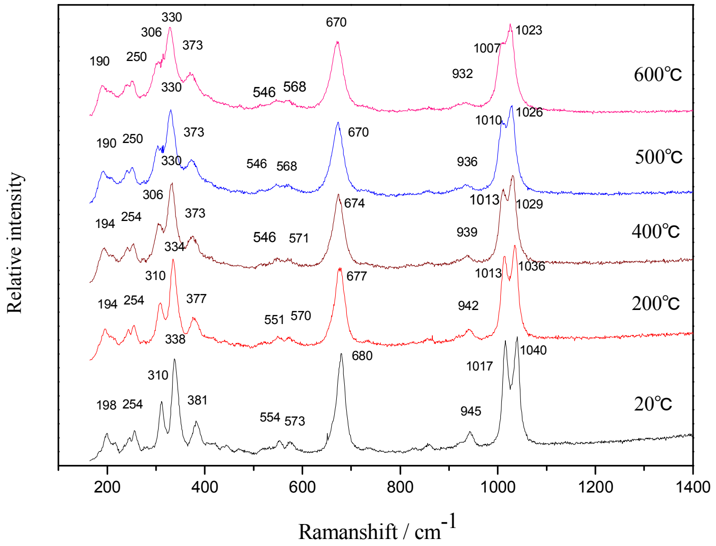

Fig.2 Raman spectra of prepared $MgSiO_3$ at varied temperatures from 20 ℃ to 600 ℃.

The frequencies of the stretching modes are related to the degree of polymerization of the SiO_4 tetrahedral network: the tetrahedra with zero (Q^0), one (Q^1), two (Q^2), and three (Q^3) bridging oxygen atoms are associated with the modes at

850, 900, 950-1000, and 1050-1100 cm^{-1}, respectively. The frequency of Si-O-Si bending vibrations in the prepared $MgSiO_3$ of this study is at around 680 cm^{-1}, while the frequency of Q^1 mode is about 945 cm^{-1}, and the frequencies of Q^2 are 1017 and 1040 cm^{-1} at ambient conditions. The typical Raman spectra of the prepared $MgSiO_3$ confirm that it has interlocking chains of silica tetrahedra, which are branched together by magnesium octahedra.

In order to obtain the details about the alkali fusion process of $MgSiO_3$, including the presence of the reaction intemediates, the alkaline fusion process of the prepared $MgSiO_3$ using sodium hydroxide was carried out under different operating conditions. The residues from the alkali fusion process followed by water washing were examined by XRD analyses. Fig.3 shows the typical XRD patterns of the residues for the alkali fusion at 600 ℃ for 30 min with varied weight ratios of NaOH to $MgSiO_3$ from 5:1 to 16:1. It can be deduced from the XRD patterns that the decomposition of $MgSiO_3$ is completed after the 30-min alkali fusion at 600 ℃ when the weight ratio of NaOH to $MgSiO_3$ is 16:1, since MgO is the only phase detected from the XRD pattern of the residue. The starting materials of NaOH and $MgSiO_3$ can be converted to $Mg(OH)_2$ and sodium silicate as final products of the alkali-fusion process, in which the latter is dissolved during water-washing and separated from the insoluable residue. In this case, MgO is a derivative of $Mg(OH)_2$ after the residue is roasted at 600 ℃ for XRD examination. It also has been found that the higher weight ratio of NaOH to $MgSiO_3$ accelerates the chemical reactions of the alkali-fusion process controlled by the law of mass action. Furthermore, Na_2MgSiO_4 can be detected from the XRD patterns for the lower weight ratios of 12:1, 10:1 and 5:1, which is one of the reaction intermediates. When the alkali-fusion process was performed at 400℃, more details about the reaction intermediates can be found. Fig.4 shows the XRD patterns of the residues from $MgSiO_3$ after the 15-min alkali-fusion process, in which $MgSiO_4$ can be recognized as another reaction intermediate besides Na_2MgSiO_4.

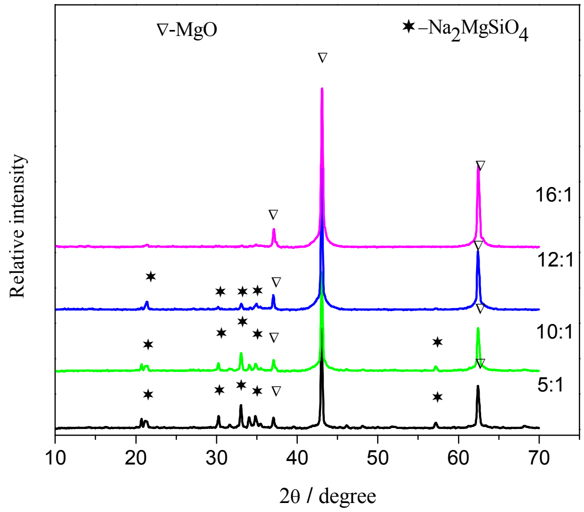

Fig.3 XRD patterns of the water-leaching residues from $MgSiO_3$ after the alkali fusion process at 600 ℃ for 30 min with the different weight ratios of NaOH to $MgSiO_3$.

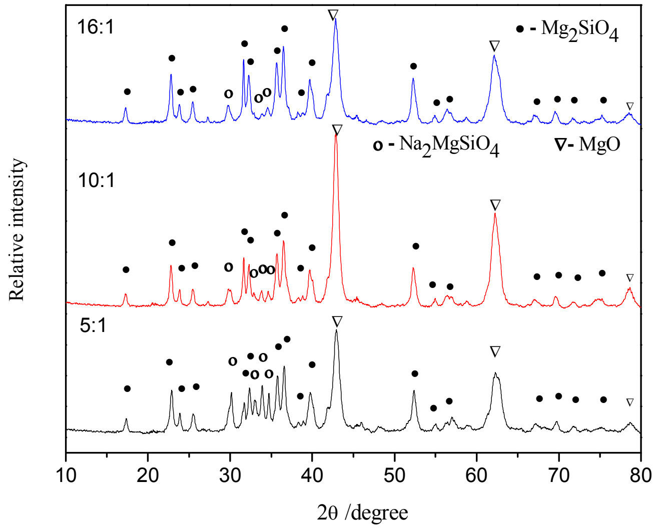

Fig.4 XRD patterns of the water-leaching residues from $MgSiO_3$ after the alkali fusion process at 400 □ for 15 min with the different weight ratios of NaOH to $MgSiO_3$ from 5:1 to 16:1.

In order to make references for distinguishing the reaction intermadiates by Raman spectroscopy in situ, Raman spectra of sodium hydroxide, which is one of the starting materials for the alkali-fusion process, are shown in Fig.5. In general, there should be no band due to the valence vibration of O-H at ~ 1080 cm^{-1} [16] if the sample of NaOH is free of sodium carbonate, while the typical band at approximately 1080 cm^{-1} due to CO_3^{2-} exists in the Raman spectra of sodium carbonate [17]. Fig.5 shows the intense band at 1076 cm^{-1} in the Raman spectrum of the NaOH sample at room temperature, and the band shifts to the lower frequency with increasing of temperature. Since all the Raman measurements were carried out at ambient conditions in this case, and sodium hydroxide could readily absorb CO_2 in the air and form sodium carbonate. The Raman spectra of the prepared Mg_2SiO_4 are shown in Fig.6 in which the bands at 859 and 894 cm^{-1} are attributed to stretching mode of Q^0 in magnesium orthosilicate. Small shifts in these band positions are also observed due to the temperature increase from 20 to 600 ℃.

The Raman spectra were collected continuously during the alkali fusion process once the reactants were heated up to the different setting temperatures at the rate of 10 ℃/min from the room temperature. Fig.7 displays the Raman spectra of the reaction mixture at different temperatures. The mole ratio of NaOH to $MgSiO_3$ in the mixture is 2:1.

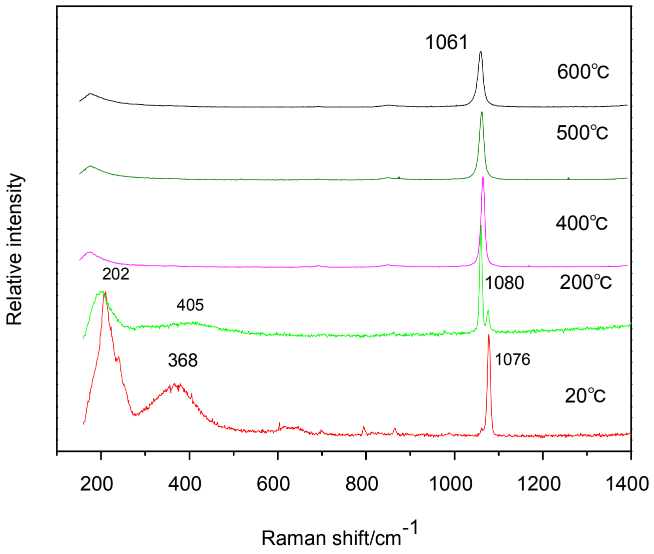

Fig.5 Raman spectra of the sample of anhydrous NaOH at different temperatures.

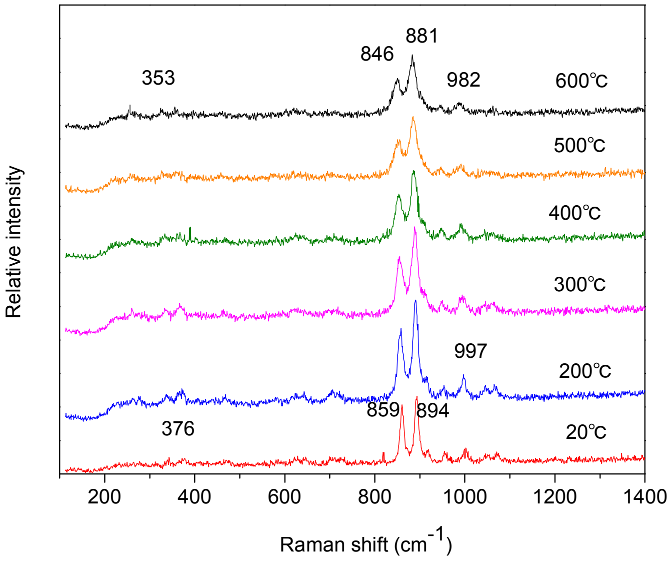

Fig.6 Raman spectra of the prepared Mg_2SiO_4 at different temperatures.

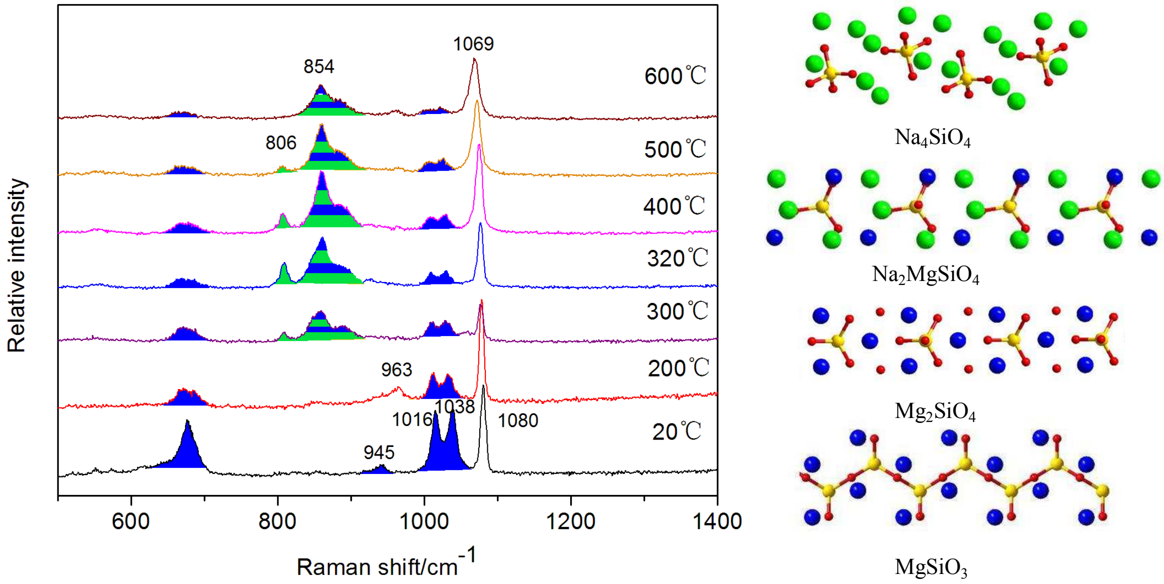

Fig.7 Raman spectra of prepared $MgSiO_3$ during the alkali fusion process as a function of the elevated temperature at the mole ratio NaOH : $MgSiO_3$ of 2:1.

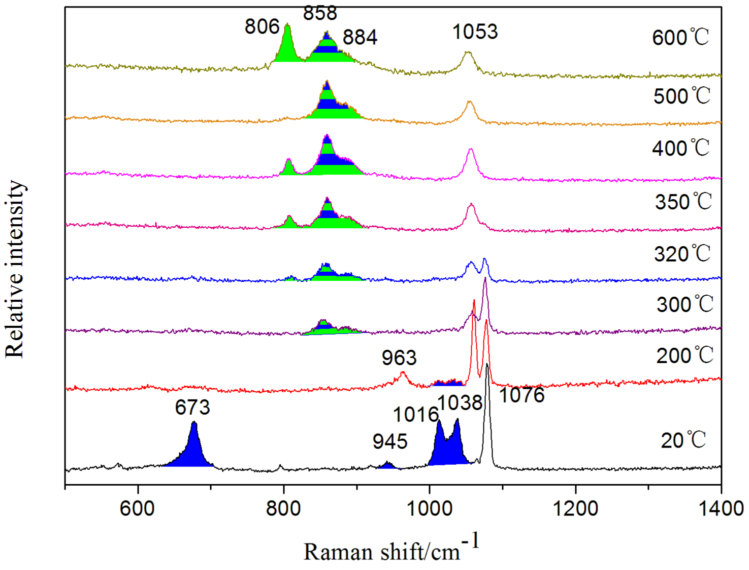

Fig.8 Raman spectra of prepared $MgSiO_3$ during alkali fusion process as a function of the elevated temperature at mole ratio NaOH: $MgSiO_3$ of 5:1

With increasing temperature, the intensity of the bands for Q^2 bending mode at 673 cm^{-1} and stretching mode at 1016 and 1038 cm^{-1} in $MgSiO_3$ decreases distinctly as the alkali fusion progresses. However, the band at ~963 cm^{-1} due to Q^2 stretching mode in Na_2SiO_3 [18] can only be found at 200 ℃, which is lower that the melt point of NaOH (318 ℃). However, the band vanishes when the alkali fusion process initiates at 300 ℃. The lifetime of Na_2SiO_3 should be very short if it were one of the intermediates for the alkali fusion process. The bands at ~850 and 890 cm^{-1} appear distinctly when the temperature rises from 300 to 600 ℃ in Fig.7. These bands are attributed to a non-bridging Si-O stretching mode in Mg_2SiO_4 [19] as also shown in Fig.6. Consequently, it can be deduced that Mg_2SiO_4 is one of the reaction intermediates, which is in good agreement with the results of the XRD analyses above. The band at around 805 cm^{-1} should be attributed to Si-O stretching mode in sodium orthosilicate (Na_4SiO_4) [20] which is a final product of the alkali fusion process. Since the magnesium atom is heavier than sodium, the vibration of Si-O stretching should appear at lower frequencies when Na acts as a network modifier instead of Mg [21]. It can be found that the chains of silica tetrahedra are disrupted gradually during the alkali fusion process, which leads to a diminishing of number of Q^2, and an increasing of Q^0 number. The variations observed on Raman spectra as the temperature rises to 300 ℃, which is near to the melt point of NaOH, are related with reorganization of the tetrahedral network. However, the bands at around 850 and 890 cm^{-1} are incorporated into a wider, less defined peak, not like the sharply separated two peaks for the pure Mg_2SiO_4. Probably, the bands for stretching mode of Q^0 in Na_2MgSiO_4 overlap with those of Mg_2SiO_4 since Na_2MgSiO_4 is the other one of reaction intermediates found in the former XRD analyses. The reaction intermediates of Mg_2SiO_4 and Na_2MgSiO_4 of the alkali fusion process could indicate that main role of NaOH during the alkali fusion process is to supply oxygen ions, then disrupt the chains of Si-O tetrahedral, and finally reconstruct the nesosilicate.

Fig.8 shows Raman spectra of the reaction mixture (the mole ratio of NaOH to $MgSiO_3$ is 5:1) at different temperatures. Comparing with the Raman spectra for the reaction mixture with the ratio of 2:1 at the same temperature in Fig.7, the intensity of the bands due to Si-O-Si vibration is much weaker, and the band at 963 cm^{-1} for Q^2 stretching mode in Na_2SiO_3 diminishes also when the temperature is higher than 300 □. Furthermore, the intensity of band due to Q^0 in Na_4SiO_4 increases more distinctly with the temperature when the ratio is bigger, even though there is discrepancy with the spectrum at 500 □, probably because of inhomogeneity of the reaction mixture. These results confirm the high molar ratio of NaOH to $MgSiO_3$ in the alkali fusion process can enhance disruption rate of the chains of silica tetrahedral, and reorganization rate of nesosilicate (Na_4SiO_4) as well.

4. Conclusions

Combining Raman spectroscopy in situ with the XRD analyses can give the reaction pathway for the decomposition of $MgSiO_3$ during the alkali fusion process using NaOH. The silica tetrahedral chains within magnesium inosilicate ($MgSiO_3$) is gradually disrupted, and nesosilicate with the isolated tetrahedral reorganized since the beginning of the alkali fusion process. Mg_2SiO_4 and Na_2MgSiO_4 are the two intermediates for the decomposition while final products are $Mg(OH)_2$ and Na_2SiO_4. It can be deduced that this decomposition could not initiate from the cation exchange reaction.

Acknowledgement

The authors gratefully acknowledge the financial support from National Program on Key Basic Research Project of China (Grant No.2007CB613603), the National Natural Science Foundation of China (Grant No 51174055) and the open research program of Shanghai Key Lab of metallurgy and materials processing in Shanghai University (2009-02).

References

[1] H. Lee, S. Kim, J. Oh. Electrochemical leaching of nickel from low-grade laterites. *Hydrometallurgy*, 2005, 77,

p263-268.

[2] S.C. Panda, L.B. Sukla, P.K. Rao, P.K. Jena. Extraction of nickel through reduction roasting and ammoniacal leaching of lateritic nickel ores. *Trans. Indian Inst. Met.* 1980, 33, p161– 165.

[3] S. Chander, V.N. Sharma. Reduction roasting/ammonia leaching of nickeliferous laterites. Hydrometallurgy, 1981, 7, p315– 327.

[4] R.R. Moskalyk, A.M. Alfantazi. Nickel laterite processing and electrowinning practice. *Miner. Eng.* , 2002, 15, 593– 605.

[5] G. Senanayake, J. Childs, B.D. Akerstrom, D. Pugaev. Reductive acid leaching of laterite and metal oxides — A review with new data for Fe(Ni,Co)OOH and a limonitic ore. *Hydrometallurgy*, 2011, 110, p13-32.

[6] Q. Guo, J. Qu, T. Qi, G. Wei, B. Han. Activation pretreatment of limonitic laterite ores by alkali-roasting method using sodium carbonate. *Miner. Eng.* 2011, 24, p825-832.

[7] Q. Guo, J.K. Qu, B. B. Han, G.Y. Wei, T. Qi. Dechromization Kinetics of Limonitic Laterite Ores by Alkali-roasting Method Using Sodium Hydroxide. *Advanced Materials Research*, 2011, 233-235, p798-804.

[8] Q. Guo, J.K. Qu, T. Qi, G.Y. Wei, B. B. Han. Activation pretreatment of limonitic laterite ores by alkali-roasting using NaOH. *International Journal of Minerals Metallurgy and Materials*. 2012, 19, p100-105.

[9] P. Novak, A. Kisic, T. Hrenar, T. Jednacak. In-line reaction monitoring of entacapone synthesis by Raman spectroscopy and multivariate analysis, *Journal of Pharmaceutical and Biomedical Analysis*, 2011, 54, p660-666.

[10] D. Reed, D. Book. Recent application of Raman spectroscopy to the study of complex hydrides for hydrogen storage. *Current Opinion in Solid State and Materials Science*, 2011, 15, p62-67.

[11] C. Fraulin, G. Rinke, R. Dittmeyer. In-Situ Laser Raman Spectroscopy Adapted to Process Conditions for Studying Cyclohexane Oxidation. *Journal of Flow chemistry*. 2013, 3, p87-91.

[12] N. Brun, I Youssef, MC Chevrel, D Chapron, C Schrauwen, S Hoppe, P Bourson, A Durand, In situ monitoring of styrene polymerization using Raman spectroscopy. Multi-scale approach of homogeneous and heterogeneous polymerization processes. *Journal of Raman Spectroscopy*. 2013, 44, p909-915.

[13] H. Boysen, F. Frey, H. Schrader, G. On the Proto- to Ortho/Clino Enstatite Phase Transformation: Single Crystal X-ray and Inelastic Neutron Investigation. *Phys. Chem. Minerals*. 1991, 17, p629-635.

[14] E. Huang, C.H. Chen, T. Huang, E.H. Lin, J. Xu. Raman spectroscopy characteristic of Ma-Fe-Ca pyroxene. *Amenrican Mineralogist*, 2000, 85, p473-479.

[15] S. Sim, K. Catalli. Compositional dependence of structural transition pressures in amorphous phases with mantle-related compositions. *Earth and Planetary Science Letters*, 2009, 283, p174-180.

[16] I.D. Zakiriyanova, V.A. Khokhlov, V.A. Kochedykov. Raman spectra and microdynamics of the hydroxide-ion in molten NaOH and NaCl-NaOH mixtures. *Journal of Molecular Liquids*, 1999,83, p153-162.

[17] H. Meekes, T. Rasing, P. Wyder, A. Janner, T.Janssen. Raman and infrared spetra of the incommensurate crystal Na_2CO_3. *Physical Review B*, 1986, 34(6), p4240-4254.

[18] P. Richet, B.O. Mysen, D. Andrault. Melting and premelting of silicates: Raman spectroscopy and X-ray diffraction of Li_2SiO_3 and Na_2SiO_3. *Phys. Chem. Minerals*. 1996, 23, p157-172.

[19] B.A. Kolesov, J.V. Tanskaya. Raman spectra and cation distribution in the lattice of olivines. *Materials Research Bulletin,* 1996, 31(8), P1035-1044.

[20] C. LIN, S. CHEN, L. LIU, Anionic structure and elasticity of Na_2O-MgO-SiO_2 glasses. *Journal of Non-Crystalline Solids, 2007*, 353, p413-425.

[21] N. Trcera, S. Rossano, M. Tarrida. Structural study of Mg-bearing sodosilicate glasses by Raman spectroscopy. *Journal of Raman spectroscopy*, 2011, 42, p765-772.

Colour graphic

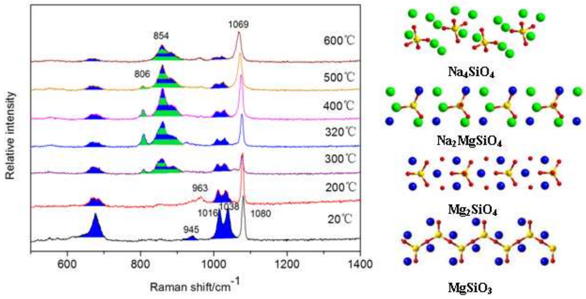

Text：

The two intermediates, Mg_2SiO_4 and Na_2MgSiO_4 reveal the reaction pathway to the alkali fusion process of magnesium inosilicate.